




# Feulgen staining applied to nuclear histomorphometry with ImageJ in canine mammary carcinoma subtypes

Coloração de Feulgen aplicada à histomorfometria nuclear com ImageJ em subtipos de carcinoma mamário canino

Arthur Perillo Rodrigues\*<sup>1</sup> , Mara Taís de Carvalho<sup>1</sup> , Hugo Henrique Ferreira<sup>1</sup> , Liliana Borges de Menezes<sup>1</sup> , Marina Pacheco Miguel<sup>1</sup> 

<sup>1</sup> Universidade Federal de Goiás (UFG), Goiânia, Goiás, Brazil 

\*corresponding author: perilloarthur34@gmail.com

Received: May 13, 2025. Accepted: September 18, 2025. Published: October 28, 2025. Editor: Luiz Augusto B. Brito

**Abstract:** Histomorphometry is an important tool in the diagnosis and prognosis of breast cancer, enabling the quantification of microscopic features related to tumor aggressiveness. This study aimed to standardize the Feulgen staining method for nuclear morphometric analysis and to compare nuclear measurements among different subtypes of canine mammary carcinoma. Histological slides with tissue microarray (TMA) sections from tubulopapillary carcinoma (TPC), complex carcinoma (CC), and solid carcinoma (SC) diagnoses were stained using the Feulgen method. Five random fields per TMA sample were photographed at 400× magnification, and nuclear morphometry was performed using ImageJ software with the *Threshold* tool. The SC subtype showed significantly larger nuclear area ( $85.40 \mu\text{m}^2 \pm 0.3159$ ) and nuclear perimeter ( $48.33 \mu\text{m} \pm 0.1217$ ) compared to the TPC and CC subtypes ( $P < 0.0001$ ). These results indicate that SC, a high-grade malignant neoplasm, presents greater nuclear dimensions. Nuclear area and perimeter proved to be more reliable parameters for comparisons between different subtypes, while circularity was useful in differentiating malignancy grades within the same subtype. Feulgen staining demonstrated high efficiency for nuclear histomorphometry, allowing precise nuclear delimitation and reducing subjectivity in quantitative evaluation.

**Keywords:** dog; histochemical staining; malignancy grade; neoplasm; nuclear morphometry.

**Resumo:** A histomorfometria é uma ferramenta importante no diagnóstico e prognóstico do câncer de mama, permitindo a quantificação de características microscópicas relacionadas à agressividade tumoral. Este estudo teve como objetivo padronizar a coloração de Feulgen para análise morfométrica nuclear e comparar as medidas nucleares obtidas entre subtipos de carcinoma mamário canino. Lâminas histológicas com cortes em microarranjos teciduais (TMA) dos diagnósticos de carcinoma tubulopapilar (CTP), carcinoma complexo (CC) e carcinoma sólido (CS) foram coradas pelo método de Feulgen. Cinco campos aleatórios por amostra de TMA foram fotografados em aumento de 400×, e a morfometria nuclear foi realizada no software ImageJ, utilizando a ferramenta *Threshold*. O subtipo CS apresentou área nuclear ( $85,40 \mu\text{m}^2 \pm 0,3159$ ) e perímetro nuclear ( $48,33 \mu\text{m} \pm 0,1217$ ) significativamente maiores em comparação aos subtipos CTP e CC ( $P < 0,0001$ ). Esses resultados indicam que o CS, neoplasia de alto grau de malignidade, apresenta maiores



dimensões nucleares. A área e o perímetro mostraram-se parâmetros mais confiáveis para a comparação entre diferentes subtipos, enquanto a circularidade auxiliou na diferenciação dos graus de malignidade dentro de um mesmo subtipo. A coloração de Feulgen demonstrou elevada eficiência para a histomorfometria nuclear, permitindo a delimitação precisa dos núcleos e reduzindo a subjetividade na avaliação quantitativa.

**Palavras-chave:** Cão; coloração histoquímica; grau de malignidade; neoplasia; morfometria nuclear.

---

## 1. Introduction

Mammary tumors are among the most frequent neoplasms in female dogs, particularly in unspayed bitches, and approximately half of these lesions are malignant <sup>(1)</sup>. Due to their high incidence and biological similarities to human breast cancer, these tumors represent a valuable model for spontaneous preclinical studies. Histologically, malignant mammary neoplasms exhibit cells with enlarged nuclei and prominent nucleoli, often accompanied by marked nuclear pleomorphism, nuclear folding, and overlapping, as well as coarse chromatin aggregates <sup>(2)</sup>. Nuclear evaluation is therefore one of the most relevant criteria in tumor diagnosis, along with histological type, mitotic index, necrosis, peritumoral and lymphatic invasion, and regional lymph node metastasis <sup>(3)</sup>.

Routine histopathological diagnosis employs hematoxylin and eosin (H&E) staining, which provides contrast between nuclear and cytoplasmic structures according to their physicochemical properties <sup>(4)</sup>. H&E staining colors most cellular organelles and extracellular matrix components in eosinophilic tones, while the nucleus, rough endoplasmic reticulum, and ribosomes appear basophilic <sup>(5)</sup>. Histochemical staining allows subjective assessment of cellular pleomorphism for grading malignancy in cancer.

Morphometric assessment of cellular and nuclear alterations is important for evaluating tumor progression. Quantitative measurements of nuclear profile, size, and shape are often correlated with malignancy <sup>(6)</sup>. In canine mammary carcinomas, metastatic lesions in regional lymph nodes have been associated with a significantly larger mean nuclear area compared to non-metastatic tumors <sup>(7)</sup>, indicating that nuclear morphometry may provide useful prognostic information. However, for accurate nuclear morphometric analysis, DNA-specific staining methods are preferred. The Feulgen reaction is a specific and sensitive histochemical technique for DNA <sup>(8)</sup>, enabling detailed visualization and measurement of nuclear structures <sup>(9)</sup>.

Considering that qualitative assessment of nuclear features is subject to interobserver variability, quantitative nuclear morphometry can provide greater objectivity in histological grading of canine neoplasms and support routine oncological diagnosis. Therefore, the present study standardized Feulgen staining for nuclear morphometric analysis and compared nuclear measurements between different subtypes of canine mammary carcinoma.

## 2. Material and methods

### 2.1 Ethical aspects and sample selection

The entire experimental analysis was approved by the Committee on Ethics in the Use of Animals (case no. 016/18). A total of 300 paraffin blocks containing fragments of canine mammary tumors were selected from a private veterinary histopathological diagnostic service, obtained from veterinary clinics between 2015 and 2018. The blocks came from samples fixed in 10 % buffered formaldehyde and subjected to routine histological processing within 48 h of receipt. The processing was performed according to a routine histological technique for paraffin embedding (dehydration, diaphanization,

impregnation, and paraffin embedding). From these blocks, new histological slides were prepared with 4 µm thick sections, which were stained with H&E according to the routine laboratory protocol described below.

As an inclusion criterion, the state of conservation of the blocks was considered (absence of cracks and good inclusion in paraffin). As exclusion criteria, blocks that exhibited diagnostic uncertainties during slide evaluation were not included.

## 2.2 Histological diagnosis and classification of breast carcinomas

Ninety-nine cases were analyzed with the following histomorphological diagnoses: 66 tubulopapillary carcinomas (TPC), 14 complex carcinomas (CC), and 19 solid carcinomas (SC). The histological classification and malignancy grade of mammary neoplasms were determined by an experienced veterinary pathologist. The classification of canine mammary neoplasms was established in accordance with the proposal by Elston and Ellis <sup>(10)</sup> and updated by Cassali <sup>(11)</sup>.

The histological malignancy grade was based on the evaluation of tubular formation, mitotic count, and nuclear pleomorphism, with each parameter assigned a numerical score (I, II, or III) <sup>(3,11)</sup>. The sum of these determined the final grade of the neoplasm <sup>(3)</sup>. Each slide was analyzed under a light microscope, using five fields to assess tubular formation and nuclear pleomorphism and ten fields to determine the mitotic count for histological grading. After defining the histomorphological diagnosis and histological grade, blocks were constructed using the tissue macroarray (TMA) technique and stained with Feulgen.

### 2.2.1 Experimental design

This is an observational, cross-sectional, and methodological study aiming to evaluate Feulgen staining as a tool for nuclear measurement. In addition, morphometric measurements were described and compared between different classifications and malignancy grades.

## 2.3 Tissue macroarray technique (TMA)

TMA blocks were prepared for each histomorphological type of canine mammary carcinoma. This technique <sup>(12)</sup> consisted of removing 0.5 to 2 mm tissue cylinders from donor paraffin blocks, which were transferred to an empty paraffin block (recipient block). Each recipient block received 50 different sample cylinders from the same histomorphological type. Renal tissue was used for localization of each case according to the map. The TMA technique allowed the analysis of a larger number of samples per slide in an optimized, standardized manner, reducing the time required for staining and analysis.

## 2.4 Feulgen staining and nuclear morphometry

The TMA slides were subjected to staining using an adapted Feulgen technique. First, the slides were dewaxed for 15 min at 60 °C and then washed in three xylene baths. Subsequently, they were immersed for 15 min in a 5 mol/L HCl solution, washed in running water, and placed in a solution containing Schiff reagent for 15 min in a darkroom. The slides were then rinsed twice in water at room temperature for 5 min each. Finally, they underwent dehydration, diaphanization, and mounting.

## 2.5 Nuclear histomorphometry

The Feulgen-stained slides were analyzed under a light microscope, and five random fields were captured using a digital camera coupled to the microscope (Leica® DMC 2900) at 400× magnification. Subsequently, nuclear evaluation was performed using ImageJ 1.52a software (National Institutes of

Health, USA), with approximately 50 nuclei per field <sup>(13)</sup>. The parameters used for nuclear morphometry were: area (the region encompassed within the nuclear perimeter); perimeter (the total length of the nuclear boundary); circularity ( $4\pi \times \text{Area} / \text{Perimeter}^2$  – describes the degree to which the nucleus approximates a perfect circle, with values approaching 1.0 indicating circularity); and Feret's diameter (the mean distance between two parallel lines tangent to the nuclear profile, representing the maximum caliper diameter).

The photomicrographs were analyzed by converting pixels to micrometers, with calibration for a 40× objective lens. All photomicrographs underwent automatic brightness adjustment. Then, the green color channel (using the split channel function) was selected, and a threshold was applied (Figure 1) to obtain a binary image converted to grayscale (nuclei stained black and the remaining image white). To delimit the area to be measured, the watershed function was applied to the binary image. Next, to exclude particles that were not representative of neoplastic nuclei, a size range of 40-170  $\mu\text{m}^2$  was predefined in the "Analyze Particles" function.

The choice of the nuclear analysis interval was based on previously published results. Values below 40.0  $\mu\text{m}^2$  were excluded to prevent confusion between neoplastic nuclei and defense cells, which have an average nuclear area of 31.9  $\mu\text{m}^2$  <sup>(14)</sup>. In addition, Simeonov's <sup>(15)</sup> study reported mean nuclear areas in canine mammary carcinomas ranging from 66.83  $\mu\text{m}^2$  to 143.71  $\mu\text{m}^2$ . These data allowed us to establish the size range of nuclei to be analyzed and considered neoplastic.

In addition to the measurement, nuclei of neoplastic epithelial cells with evident nucleoli and coarsely condensed chromatin were analyzed. Stromal cell nuclei, defense cell nuclei, and necrotic areas were not evaluated. Overlapping cells or cells with distorted morphology were also excluded from the analyses.

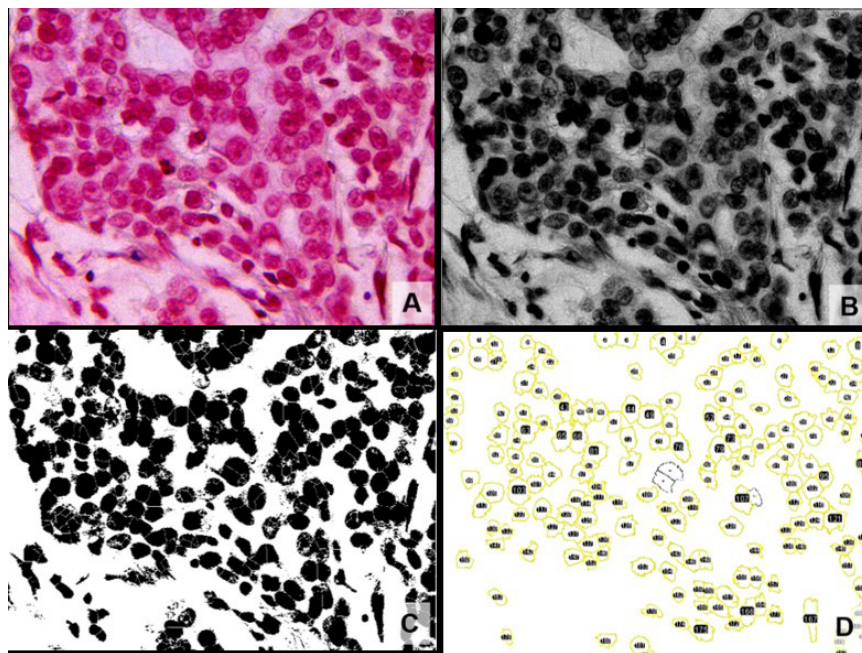


**Figure 1.** Morphometric analysis steps using ImageJ – photomicrograph of tubular carcinoma, grade II, stained with Feulgen (400× magnification). (A) Image acquisition by the software with brightness correction. (B) Selection of the image with the green color channel (Split Channels function). (C) Image after threshold adjustment and application of the particle separation process (Watershed). (D) Particles measured using the "Analyze Particles" function, with a size selection interval of 40-170  $\mu\text{m}^2$  to eliminate nuclei of defense cells (31.9  $\mu\text{m}^2$ ).



2.6 Statistical analysis

Data from the Feulgen staining nuclear measurements were presented as mean and standard deviation according to classification type and malignancy grade of the studied neoplasms. The Shapiro-Wilk normality test was applied, and ANOVA followed by Tukey’s post hoc test was used to analyze the three carcinoma classifications. Student’s t-test was used to compare different malignancy grades within the same carcinoma classification.

3. Results

The total number of cases analyzed by histomorphological classification and malignancy grade is shown in Table 1.

**Table 1.** Total histological classification and malignancy grade of canine mammary tumors

Histological classification	Malignancy grade I	Malignancy grade II	Malignancy grade III	Total
Tubulopapillary carcinoma	55	11	0	66
Complex carcinoma	14	0	0	14
Solid carcinoma	0	10	9	19

Feulgen strongly stained DNA in magenta, ensuring accurate identification and delimitation of cell nuclei compared to H&E staining. The other cellular components exhibited clear eosinophilic staining or remained unstained (Figure A2, B2, C2). Among the carcinoma types evaluated, SC and CC showed greater nuclear density and pleomorphism compared to TPC (Figure 2).

Nuclei of TPC showed moderate to marked pleomorphism, arranged in two or more rows of epithelial cells forming a tubular aspect. The chromatin was hyperchromatic and disorganized, and nucleoli were mainly located in the nuclear periphery. The epithelial and myoepithelial cells of CC were organized in tubules or irregular bundles, with central nuclei ranging from round to ovoid shapes, displaying dotted chromatin and small central nucleoli. In SC samples, the nuclei showed marked pleomorphism, distributed in solid, hyperchromatic rows or strands without a uniform pattern, with disorganized chromatin and nucleoli predominantly located at the nuclear periphery (Figure 2).

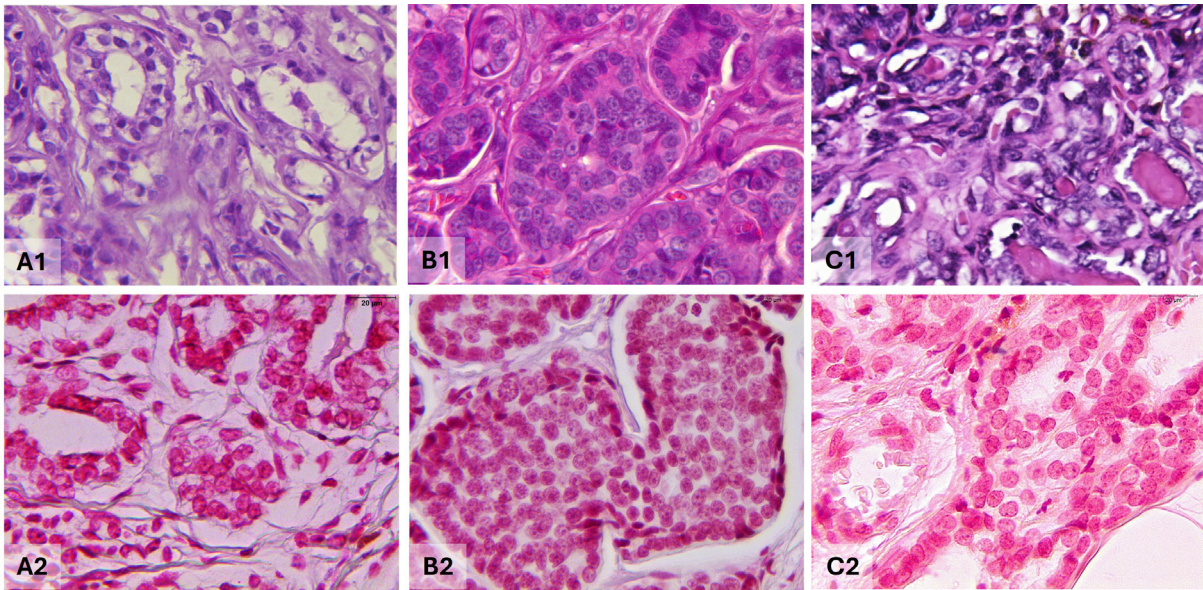


**Figure 2.** Photomicrographs of canine mammary tumors. **(A1)** Tubulopapillary carcinoma (hematoxylin and eosin, HE): neoplastic cells arranged in tubules forming papillary structures, with evident nuclear pleomorphism. **(A2)** Tubulopapillary carcinoma (Feulgen): malignant nuclei stained magenta. **(B1)** Solid carcinoma (HE): cords of cells forming solid sheets or lobules, with pleomorphic nuclei showing chromatin stippling. **(B2)** Solid carcinoma (Feulgen). **(C1)** Complex carcinoma (HE): disorganized cells lacking clear boundaries, with pleomorphic nuclei and chromatin stippling. **(C2)** Complex carcinoma (Feulgen). With Feulgen staining, nuclei are sharply distinguished from the unstained background, facilitating morphometric analysis. Magnification ×400.

A total of 25,180 nuclei were analyzed (8,878 TPC, 8,604 SC, and 7,698 CC). SC had a larger nuclear area and perimeter (Table 2) compared to CC and TPC. The Feret value was higher for TPC than for CC, but neither showed a difference from SC. Circularity in CC cells was significantly higher than in the other subtypes.

**Table 2.** Mean, standard deviation, and p-value of nuclear area, nuclear perimeter, Feret, and circularity of canine mammary tumors

Diagnosis	(p)	
Area, $\mu\text{m}^2$ (mean $\pm$ standard deviation)		
Tubulopapillary carcinoma	$77.00 \pm 0.314^a$	< 0.0001
Complex carcinoma	$80.75 \pm 0.365^b$	
Solid carcinoma	$85.40 \pm 0.316^c$	
Nuclear perimeter, $\mu\text{m}^2$ (mean $\pm$ standard deviation)		
Tubulopapillary carcinoma	$45.13 \pm 0.123^a$	< 0.0001
Complex carcinoma	$47.39 \pm 0.138^b$	
Solid carcinoma	$48.33 \pm 0.122^c$	
Feret, $\mu\text{m}^2$ (mean $\pm$ standard deviation)		
Tubulopapillary carcinoma	$13.69 \pm 0.096^a$	0.0125
Complex carcinoma	$13.44 \pm 0.031^b$	
Solid carcinoma	$13.50 \pm 0.026^{ab}$	
Circularity, $\mu\text{m}^2$ (mean $\pm$ standard deviation)		
Tubulopapillary carcinoma	$0.113 \pm 0.002^a$	< 0.0001
Complex carcinoma	$0.464 \pm 0.001^b$	
Solid carcinoma	$0.236 \pm 0.003^c$	

Mean, standard deviation and p-value of nuclear area, nuclear perimeter, Feret, and circularity of canine mammary tumors: <sup>a, b, c</sup> in the rows indicate statistical differences between groups by One-way ANOVA with Tukey's post-test at a 5 % significance level (p <0.05).

Among the malignancy grades (Table 3), grade I TPC had smaller area, perimeter, and circularity compared to grade II TPC. The Feret value was higher in grade I than in grade II. Among the SC grades, a larger area, perimeter, and Feret value were observed for grade II compared to grade III, with circularity being the only major parameter for grade III SCs. Malignancy grade analysis was not possible for CC, as all samples were grade I.

**Table 3.** Mean, standard deviation, and p value of nuclear area, nuclear perimeter, Feret, and circularity of canine mammary tumors according to malignancy grade

Diagnosis (p)	Histological grade (mean $\pm$ standard deviation)	
	<b>Area, <math>\mu\text{m}^2</math></b>	
Tubulopapillary carcinoma (p= 0.0001)	Grade I (67.34 $\pm$ 0.41)	Grade II (82.85 $\pm$ 0.42)
Solid carcinoma (p=0.0121)	Grade II (88.39 $\pm$ 0.68)	Grade III (86.36 $\pm$ 0.47)
Complex carcinoma	Grade I (80.75 $\pm$ 0,37)	---
	<b>Nuclear perimeter, <math>\mu\text{m}^2</math></b>	
Tubulopapillary carcinoma (p= 0.0001)	Grade I (41.44 $\pm$ 0.18)	Grade II (47.21 $\pm$ 0.16)
Solid carcinoma (p=0.0001)	Grade II (49.37 $\pm$ 0.28)	Grade III (48.02 $\pm$ 0.14)
Complex carcinoma	Grade I (47.39 $\pm$ 0.14)	---
	<b>Feret, <math>\mu\text{m}^2</math></b>	
Tubulopapillary carcinoma (p=0.0069)	Grade I (14.02 $\pm$ 0.25)	Grade II (13.49 $\pm$ 0.04)
Solid carcinoma (p=0.0006)	Grade II (13.66 $\pm$ 0.05)	Grade III (13.45 $\pm$ 0.03)
Complex carcinoma	Grade I (13.44 $\pm$ 0.03)	---
	<b>Circularity, <math>\mu\text{m}^2</math></b>	
Tubulopapillary carcinoma (p=0.0001)	Grade I (0.015 $\pm$ 0.002)	Grade II (0.017 $\pm$ 0.002)
Solid carcinoma (p=0.0001)	Grade II (0.149 $\pm$ 0.005)	Grade III (0.155 $\pm$ 0.004)
Complex carcinoma	Grade I (0.464 $\pm$ 0.001)	---

A significance level of 5 % (p <0.05) indicates statistical differences between groups using the t-test.

#### 4. Discussion

The present study demonstrated the applicability of Feulgen staining for nuclear morphometric analysis in canine mammary carcinomas using an open-source computer program - ImageJ. Destexhe *et al.*<sup>(16)</sup> also applied Feulgen staining to canine mammary tumors using cytocentrifuged preparations of stained nuclei to evaluate ploidy, S-phase fraction, and nuclear area in benign and malignant lesions. The study showed that the mean nuclear surface area was significantly smaller in malignant lesions (7,062  $\mu\text{m}^2$ ) compared to benign ones (7,745  $\mu\text{m}^2$ ; p < 0.05).

Although our study did not include the analysis of benign lesions, the values obtained for malignant lesions<sup>(16)</sup> were close to those described for tubulopapillary carcinoma. These findings reinforce the potential of nuclear morphometry as a complementary tool in the diagnosis and prognosis of mammary neoplasms, while also highlighting the need for future studies encompassing different histological subtypes, including benign lesions, to better elucidate the morphometric patterns associated with tumor progression.

Nuclear DNA content can be determined by image cytometry analysis (static cytometry), which can be performed by analyzing images of Feulgen-stained paraffin sections, allowing direct visualization of the analyzed cells and simultaneously analyzing morphological characteristics when flow cytometry is not possible<sup>(17)</sup>. The Feulgen reaction consists of two steps: the first is acid hydrolysis, usually performed with an HCl solution. The second step consists of treating the fragment with Schiff's reagent, a leukoderivate of basic fuchsin<sup>(8)</sup>. Several studies have reported the use of Feulgen staining and its usefulness in nuclear morphometry research<sup>(18-21)</sup>. This simple, inexpensive, and reliable histochemical method enables nuclear analysis of cancer cells, and the evaluated parameters can assist in the diagnosis of canine mammary neoplasms.

Nuclear morphometry was first introduced in humans as a prognostic parameter in prostatic adenocarcinomas in 1982 <sup>(22)</sup>, establishing its role in oncological research. Since then, advances in bioimage analysis technologies have significantly enhanced the precision and reproducibility of nuclear assessment. Image analysis systems are particularly valuable when quantitative accuracy is required, as they reduce observer-dependent variability and enable standardized data acquisition. In the biomedical field, bioimage software has become indispensable, allowing the extraction of diagnostically and prognostically relevant information from photomicrographs in a cost-effective manner <sup>(23)</sup>.

Among the most widely used platforms is ImageJ <sup>(24)</sup>, developed by the National Institutes of Health (NIH), which has gained prominence not only due to its accessibility but also because of its open-source nature, fostering community-driven innovation through plug-in development. Despite these advantages, challenges remain regarding the standardization of analytical protocols, the integration of morphometric data with clinical outcomes, and the interpretation of results across diverse tumor types.

In multicenter studies of canine mammary neoplasms, simple tubulopapillary carcinoma was reported as the most frequent malignant type (256 out of 999 cases, approximately 25.6 %) <sup>(25)</sup>. A retrospective study identified this histological subtype in 15.7 % of the analyzed tumors <sup>(26)</sup>, while epidemiological data from the Canary Islands reported frequencies ranging from 24.7 % to 29.7 % across different time periods <sup>(27)</sup>, which was also evidenced in our study.

The results of the present study demonstrate that the parameters of nuclear area and perimeter are higher in SC than in TPC or CC. In a study with similar objectives and results, but conducted with cells obtained by fine-needle aspiration biopsy, stained with Hemacolor and analyzed using Image Pro Plus, the mean nuclear area for TPC was  $89.70 \mu\text{m}^2 (\pm 15.02)$  and for SC  $111.11 \mu\text{m}^2 (\pm 28.38)$ . The mean perimeter value for TPC was  $34.47 \mu\text{m} (\pm 4.27)$  and for SC  $38.62 \mu\text{m} (\pm 6.03)$  <sup>(15)</sup>, similar to those observed in the present study. These findings demonstrate that these parameters are higher in malignant lesions as a result of increased nuclear biological activity and accumulation of abnormal genetic material during carcinogenesis <sup>(28)</sup>.

Among the types of canine mammary cancer, SC has a more aggressive biological behavior compared to TPC and CC <sup>(29)</sup>, and nuclear alterations are expected to be more evident in aggressive types, consistent with the findings of this study. Similar results were observed in a comparative study <sup>(30)</sup> of cytology in benign and malignant breast neoplasms in women, in which malignant neoplasms exhibited higher nuclear area values. Nuclear morphometry was also employed in a study of prostate cancer in dogs, which showed that nuclei of neoplastic cells were larger, with greater variation in nuclear size and shape compared to normal and hyperplastic cells <sup>(31)</sup>.

The parameter used as a form factor in this study was circularity, which demonstrated that CC cells have nuclei with shapes closer to a circle when compared to those of SC and TPC. In this study, Feret's parameter, which measures the diameter of a particle with irregular margins, demonstrated that CC nuclei were smaller than those of TPC. These two measurements indicate the degree of anisocariosis <sup>(18)</sup>, that is, the variation in nuclear size among cells of the same type. In the present study, CC nuclei were found to be more rounded and less irregular than those of the other subtypes. In a human study evaluating non-metastatic renal carcinomas, nuclear shape was described as the most important factor for predicting neoplastic recurrence, and tumors composed of more rounded nuclei had a worse prognosis <sup>(32)</sup>.



However, in another study on osteosarcomas, the authors reported that patients with large, round tumor nuclei had a better prognosis than those with small and polymorphic nuclei <sup>(33)</sup>. Considering the findings of the present study, CC showed more rounded nuclei, and among the analyzed tumor subtypes, it is not the most aggressive type nor the one associated with the worst prognosis according to the literature <sup>(1,14)</sup>. Therefore, nuclear parameters are specific to each tumor type and should be used with caution in defining prognosis, requiring further studies to optimize their application.

Regarding histological grades, TPC showed lower mean values for area, perimeter, and circularity in grade I than in grade II, which corresponds to an increase in nuclear size and accumulation of abnormal genetic material in cancers with a higher degree of malignancy <sup>(28)</sup>. In SC, the area, perimeter, and Feret values were higher in grade II than in grade III, and only circularity was lower in grade III. Our findings regarding circularity were similar to another study showing that large and round tumor nuclei were associated with a better prognosis than small, polymorphic nuclei <sup>(1,3)</sup>. Thus, circularity appears to be a good criterion for morphometric evaluation in indicating a higher degree of malignancy. However, further studies combined with clinical information would improve the understanding of the present results.

The Feulgen method, when combined with microscopy-based approaches, enables the comparison of histomorphological data, allowing the specific detection of variations in DNA content and intensity among nuclei <sup>(34)</sup>. The use of computational tools such as ImageJ, which can analyze and quantify nuclear structures, is essential to reduce the subjectivity inherent in qualitative assessments. Therefore, we argue that lesion staging and the evaluation of benign and malignant tumors should increasingly rely on methodologies that assist pathologists in minimizing diagnostic subjectivity.

Despite advances, challenges remain in standardizing protocols, harmonizing analytical approaches, and translating nuclear morphometry into routine clinical workflows. However, future prospects are promising. The integration of bioimaging analysis with artificial intelligence and deep learning is expected to overcome current limitations, enabling the automated detection of subtle morphometric variations and predictive modeling of tumor behavior. Furthermore, incorporating nuclear morphometry and Feulgen-based DNA quantification within the broader framework of digital pathology may facilitate improved reproducibility and accelerate the validation of quantitative imaging biomarkers <sup>(34)</sup>. Collectively, these developments suggest that nuclear morphometry, supported by Feulgen staining and advanced computational tools, will evolve from a supporting methodology into a core component of nuclear morphometric pathology studies.

## 5. Conclusion

Feulgen staining enabled accurate and reliable morphometric analysis of canine mammary carcinoma nuclei when combined with the ImageJ analysis tool. Carcinomas with a higher degree of malignancy had larger nuclear morphometric parameters, particularly nuclear area and perimeter. These measurements were more accurate for differentiating carcinoma types, while nuclear circularity was better for assessing malignancy grades. Although the results demonstrate morphometric distinctions between carcinoma types and malignancy grades, further investigation is needed. Studies including a larger number of cases and systematic evaluation of other malignant and benign lesions are suggested to expand these observations and provide a more comprehensive understanding of nuclear morphometric variation across the spectrum of canine mammary lesions.

### Conflicts of interest statement

The authors declare no conflicts of interest.

### Data availability statement

The data will be provided upon request.

### Author contributions

Conceptualization: A.P. Rodrigues. and M.P. Miguel. Data curation: A.P. Rodrigues. and M.P. Miguel. A Formal analysis: A.P. Rodrigues., M.T. Carvalho, and M.P. Miguel. Investigation: A.P. Rodrigues, M.T. Carvalho, H.H. Ferreira, L.B. Menezes, and M.P. Miguel. Project Administration: A.P. Rodrigues and M.P. Miguel. Resources: A.P. Rodrigues, M.T. Carvalho, H.H. Ferreira, L.B. Menezes, and M.P. Miguel. Project Administration: A.P. Rodrigues., M.P. Miguel, and L.B. Menezes. Writing (original draft, review and editing): A.P. Rodrigues, M.T. Carvalho, H.H. Ferreira, L.B. Menezes, and M.P. Miguel.

### Acknowledgments

We thank Gisleine Fernanda França and the Laboratório de Histotécnica e Inovação do Instituto de Patologia Tropical e Saúde Pública da Universidade Federal de Goiás for technical support and infrastructure for sample processing.

### Funding

This research was supported by a graduate fellowship from the National Council for Scientific and Technological Development (CNPq).

### References

1. Salas Y, Marquez A, Diaz D, Romero L. Epidemiological Study of Mammary Tumors in Female Dogs Diagnosed during the Period 2002-2012: A Growing Animal Health Problem. *PLoS One*. 2015;10(5):e0127381. <https://doi.org/10.1371/journal.pone.0127381>
2. Zink D, Fischer AH, Nickerson JA. Nuclear structure in cancer cells. *Nat Rev Cancer*. Sep 2004;4(9):677-87. <https://doi.org/10.1038/nrc1430>
3. Goldschmidt M, Pena L, Rasotto R, Zappulli V. Classification and grading of canine mammary tumors. *Vet Pathol*. Jan 2011;48(1):117-31. <https://doi.org/10.1177/0300985810393258>
4. Fischer A H, Jacobson K A, Rose J, Zeller R. Hematoxylin and eosin staining of tissue and cell sections. *CSH Protoc*. 2008 May 1;2008:pdb.prot4986. <https://doi.org/10.1101/pdb.prot4986>
5. Chan JK. The wonderful colors of the hematoxylin-eosin stain in diagnostic surgical pathology. *Int J Surg Pathol*. Feb 2014;22(1):12-32. doi: <https://doi.org/10.1177/1066896913517939>
6. Bignold LP, Coghlan BL, Jersmann HP. Cancer morphology, carcinogenesis and genetic instability: a background. *Exs*. 2006;(96):1-24. doi: [https://doi.org/10.1007/3-7643-7378-4\\_1](https://doi.org/10.1007/3-7643-7378-4_1)
7. De Vico G, Maiolino P, Cataldi M, Mazzullo G, Restucci B. Nuclear morphometry in relation to lymph node status in canine mammary carcinomas. *Vet Res Commun*. Nov 2007;31(8):1005-11. doi: <https://doi.org/10.1007/s11259-006-0108-7>
8. Mello MLS, Vidal BC. The Feulgen reaction: A brief review and new perspectives. *Acta Histochem*. Jul 2017;119(6):603-609. <https://doi.org/doi:10.1016/j.acthis.2017.07.002>
9. Lakadamyali M, Lakadamyali M. From feulgen to modern methods: marking a century of DNA imaging advances. *Histochemistry and Cell Biology* 2024 162:1. 2024-05-16;162(1). doi: <https://doi.org/10.1007/s00418-024-02291-z>
10. Elston CW, Ellis IO. Pathological prognostic factors in breast cancer. I. The value of histological grade in breast cancer: experience from a large study with long-term follow-up. *Histopathology*. Nov 1991;19(5):403-10. doi: <https://doi.org/10.1111/j.1365-2559.1991.tb00229.x>
11. Cassali GD, Lavallo GE, Ferreira E, *et al.* Consensus for the diagnosis, prognosis and treatment of canine mammary tumors-2013. 2014. <https://repositorio.ufba.br/handle/ri/5386>
12. Pires ARC, Andreiuolo FdM, Souza SRd. TMA for all: a new method for the construction of tissue microarrays without recipient paraffin block using custom-built needles. *Diagnostic Pathology*. 2006 Jul 25;1(1). doi: <https://doi.org/10.1186/1746-1596-1-14>
13. Carella F, De Vico G, Landini G. Nuclear morphometry and ploidy of normal and neoplastic haemocytes in mussels. *PLoS One*. 2017;12(3)doi: <https://doi.org/10.1371/journal.pone.0173219>
14. Papakonstantinou S, O'Brien PJ. "High Content Imaging for the Morphometric Diagnosis and Immunophenotypic Prognosis of Canine Lymphomas". *Cytometry B Clin Cytom*. Feb 28 2014;doi: <https://doi.org/10.1002/cytob.21170>
15. Simeonov R, Simeonova G. Computerized cytomorphometric analysis of nuclear area, nuclear perimeter and mean nuclear diameter in spontaneous canine mammary gland tumours. *Vet Res Commun*. Jul 2007;31(5):553-8. doi: <https://doi.org/10.1007/s11259-007-3562-y>
16. Destexhe E, Bicker E, Coignoul F. Image analysis evaluation of ploidy, S-phase fraction and nuclear area in canine mammary tumours. *Journal of Comparative Pathology*. 1995/10/01;113(3)doi: [https://doi.org/10.1016/S0021-9975\(05\)80036-2](https://doi.org/10.1016/S0021-9975(05)80036-2)

17. Cassali GD, Bertagnolli AC, Gärtner F, Schmitt F. Canine mammary tumours: A quantitative DNA study using static cytometry. *Revista Española de Patología*. 2011/10/01;44(4)doi: <https://doi.org/10.1016/j.patol.2011.05.005>
18. El Din AA, Badawi MA, Aal SE, Ibrahim NA, Morsy FA, Shaffie NM. DNA Cytometry and Nuclear Morphometry in Ovarian Benign, Borderline and Malignant Tumors. *Open Access Maced J Med Sci*. Dec 15 2015;3(4):537-44. doi: <https://doi.org/10.3889/oamjms.2015.104>
19. Yang X, Xiao X, Wu W, *et al.* Cytological study of DNA content and nuclear morphometric analysis for aid in the diagnosis of high-grade dysplasia within oral leukoplakia. *Oral Surg Oral Med Oral Pathol Oral Radiol*. Sep 2017;124(3):280-285. doi: <https://doi.org/10.1016/j.oooo.2017.05.509>
20. Kesarkar K, Tamgadge A, Peirera T, Tamgadge S, Gotmare S, Kamat P. Evaluation of Mitotic Figures and Cellular and Nuclear Morphometry of Various Histopathological Grades of Oral Squamous Cell Carcinoma: Comparative study using crystal violet and Feulgen stains. *Sultan Qaboos Univ Med J*. May 2018;18(2):e149-e154. doi: <https://doi.org/10.18295/squmj.2018.18.02.005>
21. De Potter CR, Praet MM, Slavin RE, Verbeeck P, Roels HJ. Feulgen DNA content and mitotic activity in proliferative breast disease. A comparison with ductal carcinoma in situ. *Histopathology*. Dec 1987;11(12):1307-19.
22. Diamond DA, Berry SJ, Jewett HJ, Eggleston JC, Coffey DS. A new method to assess metastatic potential of human prostate cancer: relative nuclear roundness. *J Urol*. Oct 1982;128(4):729-34. doi: [https://doi.org/10.1016/s0022-5347\(17\)53158-4](https://doi.org/10.1016/s0022-5347(17)53158-4)
23. Andrea Carlos Eduardo, Bleggi-Torres Luiz Fernando, Seixas AMTd. Análise da morfometria nuclear: descrição da metodologia e o papel dos softwares de edição de imagem. *J Bras Patol Med Lab*. 2008;44: 51-57. doi: <http://dx.doi.org/10.1590/S1676-24442008000100010>.
24. Rueden CT, Schindelin J, Hiner MC, *et al.* ImageJ2: ImageJ for the next generation of scientific image data. *OriginalPaper. BMC Bioinformatics*. 2017-11-29 2017;18(1):1-26:doi: <https://doi.org/10.1186/s12859-017-1934-z>
25. Burrai GP, Gabrieli A, Moccia V, *et al.* A Statistical Analysis of Risk Factors and Biological Behavior in Canine Mammary Tumors: A Multicenter Study. *Animals : an Open Access Journal from MDPI*. 2020 Sep 18;10(9)doi: <https://doi.org/10.3390/ani10091687>
26. Silva EMGd, Santos TRd, Silva MJB, da Silva EMG, dos Santos TR, Silva MJB. Identifying the Risk Factors for Malignant Mammary Tumors in Dogs: A Retrospective Study. *Veterinary Sciences* 2023, Vol 10, Page 607. 2023-10-05;10(10)doi: <https://doi.org/10.3390/vetsci10100607>
27. Rodríguez J, Santana Á, Herráez P, Killick DR, Monteros AEdl. Epidemiology of canine mammary tumours on the Canary Archipelago in Spain. *BMC Veterinary Research*. 2022 Jul 11;18(1)doi: <https://doi.org/10.1186/s12917-022-03363-9>
28. Howell A, Bleehen NM, Taylor PJ. Nuclear morphometry and glutathione S-transferase pi expression in breast cancer. *Oncol Rep*. 2000 May-Jun;7(3):525–528. <https://doi.org/10.3892/or.7.3.609>
29. Rasotto R, Berlatto D, Goldschmidt MH, Zappulli V. Prognostic Significance of Canine Mammary Tumor Histologic Subtypes: An Observational Cohort Study of 229 Cases. *Vet Pathol*. Jul 2017;54(4):571-578. doi: <https://doi.org/10.1177/0300985817698208>
30. Kashyap A, Jain M, Shukla S, Andley M. Study of nuclear morphometry on cytology specimens of benign and malignant breast lesions: A study of 122 cases. *J Cytol*. Jan-Mar 2017;34(1):10-15. doi: <https://doi.org/10.4103/0970-9371.197591>
31. Di Donato G, Laufer-Amorim R, Palmieri C. Nuclear morphometry in histological specimens of canine prostate cancer: Correlation with histological subtypes, Gleason score, methods of collection and survival time. *Res Vet Sci*. Oct 2017;114:212-217. doi: <https://doi.org/10.1016/j.rvsc.2017.05.007>
32. Nativ O, Sabo E, Reiss R, Moskovitz B, Melamed M, Gutman M. The role of nuclear morphometry for predicting disease outcome in patients with localized renal cell carcinoma. *Cancer*. 1995 Oct 15;76(8):1447–1452. doi: <https://doi.org/10.1002/1097-0142>
33. Andrea CE, Petrilli AS, Jesus-Garcia R, Bleggi-Torres LF, MT. A. Large and Round Tumor Nuclei in Osteosarcoma: Good Clinical Outcome. *International journal of clinical and experimental pathology*. 01/30/2011 2011;4(2)
34. Biggiogera M, Cavallo M, Casali C. A brief history of the Feulgen reaction. *Histochemistry and Cell Biology*. 2024 Apr 12;162(1-2)doi: <https://doi.org/10.1007/s00418-024-02279-9>